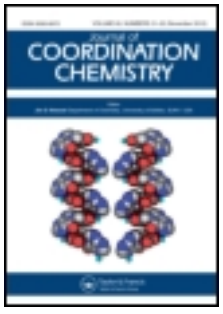

Journal of Coordination Chemistry
Publication details, including instructions for authors and subscription information:
http://www.tandfonline.com/loi/gcoo20

Syntheses and spectroscopic studies of volatile low symmetry lanthanide(III) complexes with monodentate 1H-indazole and fluorinated β-diketone

Zubair Ahmed [a], Wakeel Ahmed Dar [a] & K. Iftikhar [a]
[a] Department of Chemistry, Lanthanide Research Laboratory, Jamia Millia Islamia, New Delhi-110 025, India
Accepted author version posted online: 24 Aug 2012.Published online: 14 Sep 2012.

To cite this article: Zubair Ahmed, Wakeel Ahmed Dar & K. Iftikhar (2012) Syntheses and spectroscopic studies of volatile low symmetry lanthanide(III) complexes with monodentate 1H-indazole and fluorinated β-diketone, Journal of Coordination Chemistry, 65:22, 3932-3948, DOI: 10.1080/00958972.2012.723704

To link to this article: http://dx.doi.org/10.1080/00958972.2012.723704

Journal of Coordination Chemistry
Vol. 65, No. 22, 20 November 2012, 3932–3948

Syntheses and spectroscopic studies of volatile low symmetry lanthanide(III) complexes with monodentate 1*H*-indazole and fluorinated *β*-diketone†

ZUBAIR AHMED, WAKEEL AHMED DAR and K. IFTIKHAR*

Department of Chemistry, Lanthanide Research Laboratory, Jamia Millia Islamia, New Delhi-110 025, India

(*Received 23 November 2011; in final form 27 July 2012*)

Synthesis, photoluminescence, 4f–4f absorption, and NMR studies of highly volatile nine-coordinate complexes $[Ln(hfaa)_3(L)_3]$ (Ln = La, Pr, Nd, and Sm; hfaa is the anion of 1,1,1,5,5,5-hexafluoro-2,4-pentanedione and L = 1*H*-indazole) are described. NMR spectra reveal that three L are attached to the metal. The chemical shifts of *β*-diketonate and *H*ind protons are in opposite directions and the lanthanide induced paramagnetic shifts are dipolar. The low molecular symmetry of the complexes leads to intense luminescence with prominent Stark splitting of the bands and high oscillator strength of the hypersensitive transition. The band shape of the $^4G_{5/2}$, $^2G_{7/2} \leftarrow {}^4I_{9/2}$ transition of neodymium is similar to that of nine-coordinate complexes. Coordinating solvents have pronounced effect on the oscillator strength and band shape. The experimental intensity parameter (η_{Sm}) for the samarium complex is calculated and analyzed. The complexes could be used as precursors for high-performance lanthanide-based materials through chemical vapor deposition.

Keywords: Lanthanide; 1*H*-Indazole; NMR; 4f–4f Absorption; Luminescence

1. Introduction

Interest in photophysical properties of the lanthanide complexes intensified after Lehn's proposition that these complexes could be light-conversion molecular devices. He coined the term antenna effect to denote the UV- to visible light conversion involving distinct absorbing (ligands) and emitting (lanthanide ion) components of supramolecular species [1]. The antenna ligands transfer energy to emissive levels of lanthanide ions, thus overcoming very small absorbing coefficients of these ions. Luminescent lanthanide complexes may find applications, such as luminescent labels in fluoroimmunoassays [2, 3], lasers [4], probes and sensors for natural medical sciences [5, 6], liquid crystalline materials, and cheaper phosphors for fluorescent lighting [7–9]. Luminescent properties of lanthanide complexes and their applications have recently been reviewed [10].

*Corresponding author. Email: kiftikhar@jmi.ac.in
†Abstracted in part from the PhD thesis of Zubair Ahmed, Jamia Millia Islamia (2011).

ISSN 0095-8972 print/ISSN 1029-0389 online
http://dx.doi.org/10.1080/00958972.2012.723704

The β-diketones have strong absorptions within a large wavelength range for their π–π* transition and consequently have been targeted for their ability to sensitize luminescence of Ln(III) [10, 11]. Being coordinatively unsaturated these lanthanide tris-β-diketonates easily bind to one or more ancillary ligands to achieve higher coordination numbers [8, 12–21]. As a consequence, numerous applications of luminescent lanthanide β-diketonates have flourished in functional materials [22] and biological science [23]. The applications take advantage of unique properties of trivalent lanthanides such as sharp and easily recognizable f–f transitions almost independent of the nature of chemical environment while the excited state lifetime is long enough to allow time resolved detection [21], with excellent light harvesting properties. Lanthanide β-diketonate adducts with 2,2′-bipyrimidine [8, 15, 19] are used to design magnetic materials [24] and luminescent active materials for organic light-emitting diodes (OLEDs) [25], particularly white light OLEDs [8]. Reports describing luminescence properties of lanthanide β-diketonates using monodentate heterocyclic ligands remain scarce. Therefore, we have initiated a study of trivalent lanthanide complexes of hexafluoroacetylacetone (Hhfaa) and 1*H*-indazole (*H*ind). The hfaa was chosen for two reasons: (i) to ensure complex solubility in organic solvents and (ii) the presence of fluorines at the two terminal sides increase the residual acidity of the Ln(III) ions making them better complexing sites for incoming donors.

*H*ind acts mainly as a monodentate protonated ligand in metal complexes. With a fused aromatic ring it can be regarded as a rigid phenyl-substituted pyrazole. 1*H*-indazole and its derivatives are biologically significant [26, 27]. 1*H*-indazole (*H*ind) coordinates *via* the pyridine-type nitrogen with the pyrrole-type nitrogen usually involved in hydrogen-bond formation. In many cases, these hydrogen bonds dictate interesting molecular packing. A large number of transition metal complexes with *H*ind as well as its derivatives have been reported [25–27]. Complexes of *H*ind with trivalent lanthanides are not reported.

The main objectives of this study were to synthesize seven-coordinate complexes of trivalent lanthanides with 1,1,1-hexafluoro-2,4-pentanedione and 1*H*-indazole. Seven-coordinate complexes are expected to be of low molecular symmetry and strong luminescent complexes. In this article, we report the synthesis, paramagnetic NMR, 4f–4f absorptions, and photoluminescence properties of lanthanide complexes with hexafluoroacetylacetonate, Hhfaa, and monodentate 1*H*-indazole.

2. Experimental

2.1. *Materials*

Commercially available chemicals that were used without purification are: Ln_2O_3 (Ln = La, Pr, Nd, and Sm; 99.9%) from Aldrich. Hexafluoroacetylacetone, Hhfaa, was purchased from Lancaster and 1*H*-indazole from Koch-Light, England. The solvents used in this study were either AR or spectroscopic grade. Oxides were converted to the corresponding chlorides $LnCl_3 \cdot nH_2O$ ($n = 6$–7) by dissolving the oxides in minimum conc. HCl. It was then diluted with water and evaporated to near dryness on a water bath. This process of adding water and then evaporating to near dryness was repeated

several times until the pH of the solution is between 4 and 6. The chloride solution was finally evaporated to dryness and kept in a desiccator.

2.2. *Methods*

Elemental analyses were performed at the Chemistry Department, Banaras Hindu University, India. The melting point of the complexes were recorded by conventional capillary method as well as on a DSC instrument (DSC 6220 from SIINT, Japan) in aluminum pans with a heating rate of $10^{\circ}C\,min^{-1}$. Infrared (IR) spectra were recorded on a Perkin-Elmer spectrum RX I FT-IR spectrophotometer as KBr discs from 4000 to $400\,cm^{-1}$. Thermal analyses of the complexes were carried out on Exstar 6000 TGA/DTA and DSC 6220 instruments from SIINT, Japan with a heating rate of $10^{\circ}C\,min^{-1}$. NMR spectra were recorded on a BRUKER AVANCE II 400 NMR Spectrometer. Steady state luminescence and excitation spectra were recorded on Jobin Vyon Fluorolog 3–22 spectrofluorometer with a 450 W Xenon lamp as the excitation source and R–928 P Himamatsu photomultiplier tube as detector using a 1 cm stoppered quartz cuvette. A Voigt function was chosen by using Peak Fit v 4.12 (Jandel Software, Inc.) to fit the peaks to determine the peak center maximum, full-width at half-maximum (fwhm or peak width), and peak area. Electronic absorption spectra of the complexes were recorded on a Perkin-Elmer Lambda-40 spectrophotometer in a series of non-aqueous solvents (chloroform, dichloromethane, methanol, ethanol, nitromethane, and pyridine). The samples were contained in a $1\,cm^3$ stoppered quartz cell.

2.3. *Synthesis of the complexes*

All complexes were synthesized by a similar one step *in situ* method. The synthesis of $[La(hfaa)_3(Hind)_3]$ given here is representative.

A solution of Hhfaa (1.486 g, 7.1 mmol) in ethanol (5 mL) was added to 0.53 mL (0.1216 g, 7.1 mmol) 25% ammonia solution. This mixture in a 50 mL beaker was covered until the smell of ammonia disappeared. To this was added 5 mL ethanol solutions of *H*ind (0.2811 g, 2.3 mmol) and $LaCl_3 \cdot 6H_2O$ (0.8841 g, 2.3 mmol). The reaction mixture was stirred at room temperature for 5 h. A white precipitate of NH_4Cl (which does not melt up to 300°C) appeared during stirring and was filtered off repeatedly. The filtrate, thus obtained, was covered and left for slow evaporation at room temperature. Colorless crystals appeared after three days, which were filtered off and washed with CCl_4. The compound was recrystallized twice from ethanol and dried under *vacuum* over P_4O_{10}. Similar procedure was employed to synthesize other complexes, given in table 1.

Table 1. Characterization data of complexes, found (calculated).

Compound	Color	m.p. (°C)	% Yield	%C	%H	%N
$[La(hfaa)_3(Hind)_3]$	white	93	28	39.01 (38.69)	1.96 (1.89)	7.30 (7.52)
$[Pr(hfaa)_3(Hind)_3]$	green	95	26	39.07 (38.64)	2.03 (1.88)	7.37 (7.50)
$[Nd(hfaa)_3(Hind)_3]$	lilac	100	28	38.79 (38.51)	1.94 (1.88)	7.25 (7.48)
$[Sm(hfaa)_3(Hind)_3]$	white	99	29	38.76 (38.29)	1.96 (1.86)	7.20 (7.44)

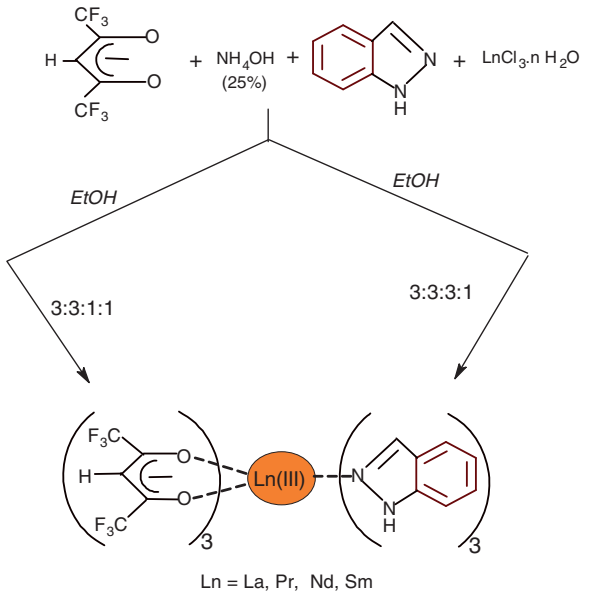

Scheme 1. Pathway for syntheses of the complexes (Ln = La, Pr, Nd, and Sm).

3. Results and discussion

The hydrated lanthanide chloride, hexafluoroacetylacetone, ammonium hydroxide (25% ammonia), and *H*ind in 1 : 3 : 3 : 1 molar ratios in ethanol were mixed in a single pot at room temperature (scheme 1). The stoichiometry was based on the assumption that seven-coordinate complexes of the type [Ln(hfaa)$_3$(*H*ind)] would be formed in line with [Ln(fod)$_3$(pz)] [28] and [Ln(fod)$_3$(im)] [29] (pz = pyrazole and im = imidazole). Instead nine-coordinate complexes were isolated. The yield of the complexes is very low since three *H*ind units are coordinated to lanthanides. The poor yield prompted us to re-investigate the synthesis. The reaction was carried out in 1 : 3 : 3 (Ln : Hhfaa : *H*ind) molar ratio under similar conditions (scheme 1), increasing the yield from 28% to 78%. These lighter lanthanides (La, Pr, Nd, and Sm) are larger, accommodating three *H*ind and three hfaa units. The stoichiometry is confirmed by elemental analyses, NMR, and ESI-MS$^+$ spectra. These complexes melt at lower temperature (93–100°C) than *H*ind (150°C). The melting point of the resulting complexes itself supports the formation of these higher coordination number complexes. The formation of higher coordination number complexes gets support from the earlier reports on hfaa complexes [14, 17]. It could be related to the higher inductive effect of the CF_3 groups at the two terminals of hfaa making the lanthanide more acidic and a better complexing site for incoming donors. The complexes are air and moisture stable and highly soluble in common organic solvents.

3.1. *Thermal studies*

The thermograms of the complexes, recorded under dinitrogen with a heating rate of 10°C min^{-1}, are similar in shape and show one step weight loss which is consistent with

vaporization (figure S1 in the "Supplementary material" section). Thus, these complexes are volatile like other hfaa complexes [17]. The total weight loss for the complexes is 99.8%. The DTA curve of the complexes displays two endothermic peaks; one between 93°C and 100°C corresponds to melting and the other at 175°C and 210°C is consistent with volatilization.

3.2. *IR spectra*

The IR spectra of complexes exhibit very strong bands around 1620 and 1520 cm^{-1} assigned to C=O and C=C stretching modes, respectively, and are typical of lanthanide tris β-diketonates [30]. The spectra of the complexes show coordinated *H*ind. The spectrum of *H*ind shows the N–H frequency as a relatively weak band at 3410 cm^{-1}, becoming a sharp strong band at 3405 cm^{-1} in the complexes. The observed shift and strong N–H band suggest interaction of ring nitrogen with lanthanide in these complexes [31].

3.3. *Mass spectra*

ESI-MS spectra of the complexes in positive mode were studied in chloroform solution. The intact molecular ion peaks are observed for all the complexes, confirming formation of the nine-coordinate complexes. The ESI-MS spectra of the complexes (figures S2–S5 in the "Supplementary material" section) show peaks at $m/z = 1115.41$, 1117.15, 1121.41, and 1126.32, which are assigned to intact molecular ions, $[La(hfaa)_3(Hind)_3 + H^+]^+$, $[Pr(hfaa)_3(Hind)_3 + H^+]^+$, $[Nd(hfaa)_3(Hind)_3 + H^+]^+$, and $[Sm(hfaa)_3(Hind)_3 + H^+]^+$, respectively. No peak corresponding to $[Ln(hfaa)_3 + H]^+$ is observed, indicating that *H*ind units are tightly held to metal ions. The other peaks observed in the spectrum may account for the diverse ionic species formed due to the fragmentation, ligand exchange, and redistribution in the vapor phase [32, 33].

3.4. *NMR spectra*

NMR spectra of the ligand and complexes (La, Pr, Nd, and Sm) were recorded in $CDCl_3$ and solutions were sufficiently concentrated (4–5 mg per 0.50 mL). Assignment of the resonances is based on spin–spin splitting and the relative intensities of the signals. The chemical shifts and the paramagnetic shifts ($\Delta\delta$) are given in table 2. The NMR spectrum of *H*ind displays six resonances of equal intensity. The broad singlet and a sharp singlet at 10.65 (bs) and 8.10 (s) ppm (δ) are assigned to N–H and H-1 of the ligand. Signals due to benzene are at 7.73 (d; H-5), 7.48 (d; H-2), 7.35 (t; H-4), and 7.15 (t; H-3). The spectrum of the diamagnetic $[La(hfaa)_3(Hind)_3]$ displays (figure 1) six signals in intensity ratio of 1 : 1 : 1 : 2 : 1 : 1. The signal at 6.01 ppm (δ) which integrates for three protons is assigned to methine of hfaa. Signals due to coordinated *H*ind are observed at 11.12 (bs; N–H), 7.89 (s; H-1), 7.72 (d; H-5), 7.47 (H-3 and H-4), and 7.19 (multiplet; H-2) ppm (δ). The substantial shift of the N–H and H-1 resonances of *H*ind, in the complex, is consistent with coordination with lanthanum. The intensity ratio of 3 : 18 between the methine (β-diketonate) and *H*ind resonances confirms that three *H*ind

Table 2. Chemical shifts and paramagnetic shifts ($\Delta\delta$) of [Ln(hfaa)$_3$(*H*ind)$_3$].[ab]

	Compound	NH	H(1)	H(2)	H(3)	H(4)	H(5)	CH
	1*H*-indazole	10.7	8.1	7.46	7.14	7.38	7.74	–
1	[La(hfaa)$_3$(*H*ind)$_3$]	11.12	7.89	7.20	7.47	7.48	7.72	6.01
2	[Pr(hfaa)$_3$(*H*ind)$_3$]	−16.56	−3.74	3.99	4.77	4.62	2.05	19.77
		(−27.68)	(−11.63)	(−3.21)	(−2.70)	(−2.86)	(−5.67)	(13.76)
3	[Nd(hfaa)$_3$(*H*ind)$_3$]	−1.01	3.91	6.60	6.31	6.22	5.40	11.23
		(−12.13)	(−3.98)	(−0.60)	(−1.16)	(−1.26)	(−1.82)	(5.22)
4	[Sm(hfaa)$_3$(*H*ind)$_3$]	9.07	7.47	7.20	6.99	7.08	7.44	7.24
		(−2.05)	(−0.42)	(0.00)	(−0.48)	(−0.40)	(−0.27)	(1.23)

[a]Chemical shifts are relative to internal Me_4Si and are expressed in ppm (δ). Positive shifts are downfield and negative shifts are upfield.
[b]The values given in parentheses are the paramagnetic shifts ($\Delta\delta$). The paramagnetic shift is the difference between the chemical shift of the nucleus in the paramagnetic complex and the corresponding shift in the diamagnetic complex.

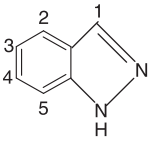

1*H*-indazole

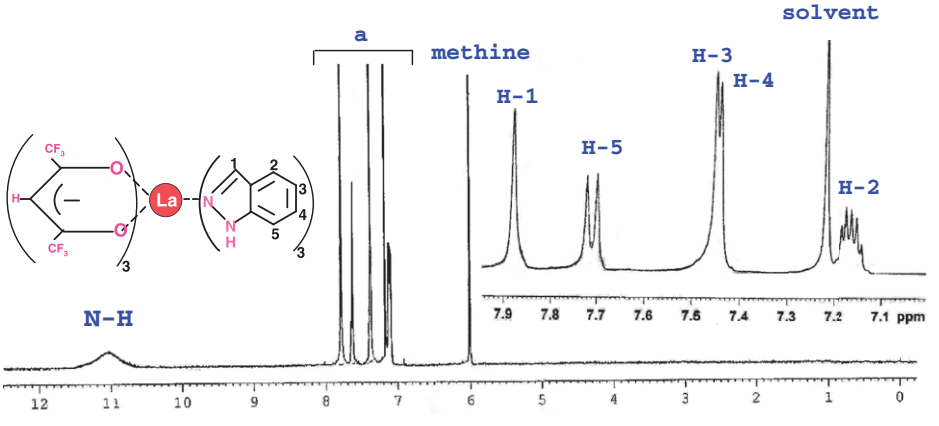

Figure 1. 400 MHz ^{1}H NMR spectrum of [La(hfaa)$_3$(*H*ind)$_3$] in $CDCl_3$. Inset (a): higher resolution of region from 7.0 to 8.0 ppm (δ).

units are attached to La(III) along with three units of hexafluoroacetylacetones, making the lanthanum(III) nine-coordinate.

The resonances of coordinated hfaa and *H*ind for paramagnetic Pr and Nd complexes are greatly shifted from their positions in the diamagnetic analog due to the large magnetic anisotropy of the lanthanides, a result of through-space dipolar interaction. Of the three lanthanide complexes (Pr, Nd, and Sm) largest upfield shifts are noted for the praseodymium complex followed by the Nd and are very small for samarium. The N–H signal of *H*ind for the praseodymium complex (figure S6 in the "Supplementary material" section) is substantially upfield shifted, as a relatively broad signal at −16.56 ppm (δ). The sharp strong signal at 19.77 ppm (δ) is assigned to methine

proton of hfaa, which is significantly downfield shifted. Thus, the Pr complex covers a chemical shift range of 36.33 ppm (δ). The strong signals at −3.74(s), 2.05(s), 3.94(d), 4.62(s) and 4.77(s) ppm (δ) are assigned to H-1, H-5, H-3, H-4 and H-2, respectively. The NMR spectrum of neodymium complex (figure S7 in the "Supplementary material" section) displays a broad signal at −1.01 for the N–H proton of the *H*ind while strong singlet at 11.23 is assigned to the methine proton of hfaa. H-1 resonates as a sharp singlet at 3.91 while H-5 appears as a doublet at 5.40 ppm (δ). H-2 and H-4 appear as independent signals at 6.31 and 6.22 ppm (δ), respectively. The triplet at 6.60 ppm (δ) is assigned to H-3. The chemical shift range covered in the neodymium complex is only 12.23 ppm (δ). The much larger upfield shifts of the protons produced by praseodymium is at the expense of resolution since the fine structures disappear from the resonances of H-2, H-4, and H-5. The loss of fine structure could be related to paramagnetically enhanced relaxation of these nuclei due to larger anisotropy in the susceptibility.

An interesting feature of the spectra of the paramagnetic complexes is the signal position of the methine resonance. The three metals (Pr, Nd, and Sm) are known as upfield shifters and have shifted the resonances of coordinated *H*ind to higher fields compared to their position in the diamagnetic complex. However, the methine resonance of hfaa has moved downfield and has its sign opposed to that of paramagnetic shift of aromatic protons, reflecting the important role of geometry of the complex in solution and thereby significance of the geometric factor ($3\cos^2\theta - 1$) in deciding direction of the shifts in a given complex which decrease with increasing distance of the proton from the metal ion. The result reflects that the paramagnetic shifts in these complexes are dominated by dipolar interaction, strongly supported by observations on [Ln(fod)$_3$phen] [34] and [Ln(hfaa)$_3$phen] [17] complexes (where fod is 6,6,6,7,7,8,8,8-heptafluoro-2,2-dimethyl-3,5-octandione).

3.5. *The 4f–4f absorption properties*

Intensity of the absorption is measured by its oscillator strength (P) which is directly proportional to the area under the absorption band and can be evaluated from equation (1) [35],

$$P = 4.31 \times 10^{-9}\left[\frac{9\eta}{(\eta^2+2)^2}\right]\int \varepsilon(\nu)\mathrm{d}\nu, \tag{1}$$

where ν is the energy of the transition in cm^{-1}, ε is the molar extinction coefficient, and η is the refractive index of the solution. The oscillator strengths of the transitions were determined by evaluating area under the peak.

3.5.1. [Nd(hfaa)$_3$(Hind)$_3$]. Absorption properties of the complex are studied in a series of non-aqueous solvents (chloroform, dichloromethane, methanol, ethanol, nitromethane, and pyridine). Absorption spectra of Hhfaa and *H*ind and neodymium complex in chloroform are dominated by spin allowed π–π^* transitions of Hhfaa and *H*ind in the ultraviolet region (200–400 nm). *H*ind and Hhfaa show a strong absorption at 276 and 275 nm, respectively. The spectrum of the complex contains essentially the combined ligand absorptions at 292 nm, shifted to longer wavelength (red-shift) as compared to

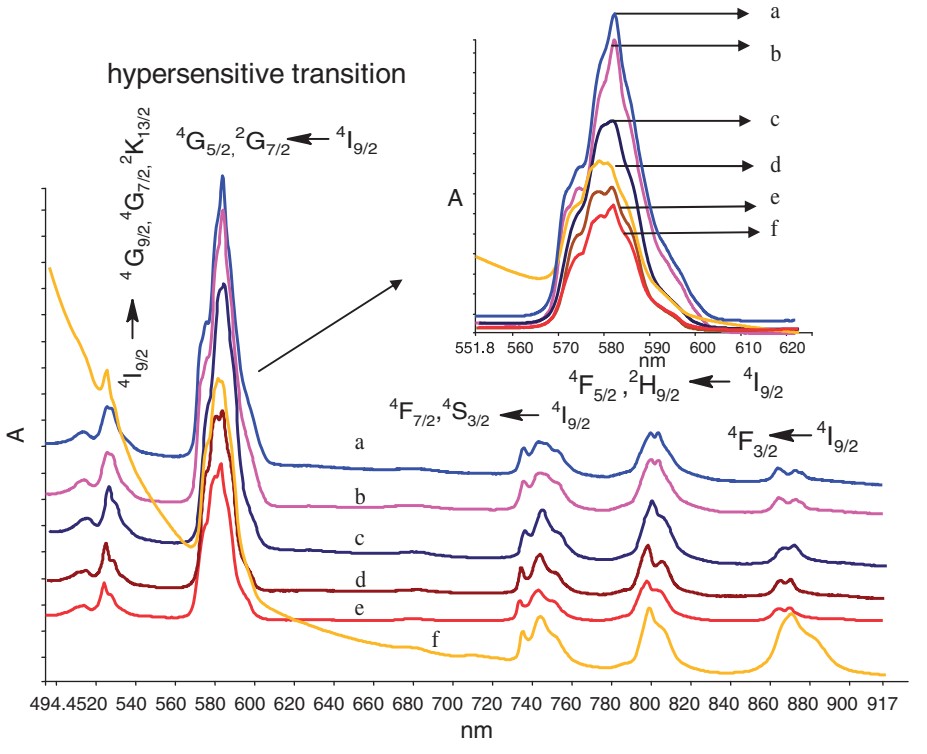

Figure 2. 4f–4f absorption spectra of nine-coordinate $[Nd(hfaa)_3(Hind)_3]$ (concentration = 5×10^{-3} mol L^{-1}): (a) chloroform (blue), (b) dichloromethane (pink), (c) nitromethane (navy), (d) methanol (brown), (e) ethanol (red), and (f) pyridine (orange).

free ligands (figure S8 in the "Supplementary material" section), and demonstrates stabilization of π-orbitals after coordination of the ligands to neodymium. Absorption spectra of $[Nd(hfaa)_3(Hind)_3]$, in the visible region, contain eight multiplet-to-multiplet transitions originating from $^4I_{9/2}$ ground state to the various excited states (figure 2 and table 3). The transition $^4G_{5/2} \leftarrow {}^4I_{9/2}$ located near the middle of the visible region is *very intense* and overlapped by a less intense transition $^2G_{7/2} \leftarrow {}^4I_{9/2}$. The relatively high intensity and unusual sensitivity to the chemical environment about the neodymium ion of this transition have led to its classification as *hypersensitive*; its behavior is in sharp contrast to many other typically weak and consistently unvaried normal f–f transitions [29, 36–39]. Its intensity and band shape have been used as qualitative indication of symmetry, coordination number, and number of neodymium metal ions present in a complex [15–19, 29, 39, 40]. The oscillator strengths of the transitions, determined using equation (1), in various coordinating and non-coordinating solvents along with the oscillator strength of aqueous $NdCl_3$ are collected in table 3. The oscillator strength of the $^4G_{5/2}$, $^2G_{7/2} \leftarrow {}^4I_{9/2}$ hypersensitive transition in any solvent is much larger than the oscillator strength of aqueous $NdCl_3$. This huge enhancement in the oscillator strength of this transition of the complex is attributed to the polarizability of the β-diketone and heterocyclic ligands and anisotropy of this polarizability [37]. The intensity of the hypersensitive transition mainly depends on the symmetry of the lanthanide complex,

Table 3. Oscillator strength of [Nd(hfaa)$_3$(*H*ind)$_3$] in various solvents.

$S'L'$ J' Transitions Nd^{3+} ($\leftarrow {}^4I_{9/2}$)		Spectral ranges[a] (cm^{-1})	Nd^{3+} aqua-ion[b] ($P \times 10^6$)	Oscillator strength ($P \times 10^6$)					
				A	B	C	D	E	F
$^4F_{3/2}$	Nd-I	10,921–11,761	1.26	1.81	1.91	2.35	1.89	2.27	1.82
$^4F_{5/2}$, $^2H_{9/2}$	Nd-II	11,910–12,880	7.84	8.28	7.24	7.66	6.99	8.18	8.46
$^4F_{7/2}$, $^4S_{3/2}$	Nd-III	12,911–13,890	7.90	7.78	6.88	7.08	6.30	6.63	6.61
$^4F_{9/2}$	Nd-IV	14,228–15,121	0.36	0.97	0.52	0.38	0.62	0.56	6.22
$^4G_{5/2}$, $^2G_{7/2}$	Nd-V	16,389–17,770	8.60	78.00	74.00	40.70	49.50	65.44	38.90
$^4G_{7/2}$, $^4G_{9/2}$, $K_{13/2}$	Nd-VI	18,169–20,098	6.20	14.28	12.84	7.53	9.34	12.70	3.34
$^4G_{11/2}$, $^2G_{9/2}$, $^2K_{15/2}$, (^2D,^2P)$_{3/2}$	Nd-VII	20,407–22,063	1.09	0.62	0.38	0.61	0.74	0.79	0.66
$^2P_{1/2}$ $^2D_{5/2}$	Nd-VIII	22,207–23,507	0.35	0.24	1.73	0.12	0.15	0.16	0.14

A: chloroform; B: dichloromethane; C: methanol; D: ethanol; E: nitromethane; F: pyridine.
[a]The spectral ranges observed for the transitions vary from solvent to solvent, so the values listed here are only meant to indicate approximate location of the bands.
[b]Taken from ref. [41].

the polarizability of the ligands, and the degree of covalency of Ln–L bonds. The largest intensification is noted in non-coordinating solvents (chloroform and dichloromethane). The oscillator strengths are much lower in coordinating solvents, pointing toward complex-solvent interactions. The lower values could be the result of coordination of a solvent molecule which changes the coordination number of Nd from nine to ten and a less symmetric structure is transformed into a more symmetric one, resulting in decrease of the oscillator strength of the hypersensitive transition; solvent coordination is without displacement of *H*ind since dissolution of the complex in coordinating solvent results in striking change in the shape of the absorption band due to hypersensitive transition. When solvent molecules coordinate by displacing the original ligands from inner coordination sphere and the coordination number remains unaltered, the band does not change its shape [39]. Among the coordinating solvents, largest intensification is noted for nitromethane, followed by ethanol and methanol, implying that ethanol as a stronger donor intensifies the band more effectively than methanol.

Comparing the oscillator strength of the hypersensitive transition of the present complex with those observed for analogous nine-coordinate hfaa complexes, [Nd(hfaa)$_3$(tptz)] (where tptz is 2,4,6-tris(2-pyridyl)-1,3,5-triazine) (49.00×10^6) [18], and eight-coordinate [Nd(hfaa)$_3$(phen)] (61.74×10^6) [17], we note higher oscillator strength for the complex under study. The higher value as compared to the eight-coordinate phen complex could be argued from symmetry. Since a nine-coordinate complex is more asymmetric than the symmetric eight-coordinate complex, the low molecular symmetry is responsible for higher oscillator strength. However, among the present *H*ind and earlier reported tptz complexes, both of which are nine-coordinate, the higher oscillator strength of the *H*ind complex could not be explained by symmetry alone. The tridentate tptz (p*K*a = 3.10) is more basic and relatively more rigid than the less basic flexible *H*ind (p*K*a = 1.25), imparting more asymmetry around neodymium and therefore, higher oscillator strength. The experimental result is reverse of the prediction. Thus, it is clear that besides symmetry of the field, basicity of the ligands also contributes in oscillator strength. There are three *H*ind units and the sum total of the p*K*a of the three units is 3.75, which is larger than the p*K*a of tptz. Thus, joint effect

of the three *H*ind would bring greater covalency in their bonding. These results indicate that the combined effect of three *H*ind is more effective in promoting 4f–4f electric–dipole intensity than a single tptz. It is, therefore, reasonable to associate this increase with ligand basicity as proposed by Henrie *et al*. in their theory of hypersensitivity [38].

3.5.2. Band shape. Both band shape and intensity of the hypersensitive transition have been used as qualitative indications of symmetry [15–19, 29, 39–41]. The changes in band shape of hypersensitive and non-hypersensitive transitions as the environment (solvent) around Nd(III) is varied are shown in figure 3. Chloroform and dichloromethane are non-coordinating solvents and the band shape of the transitions in these solvents is identical and may be considered as the standard band shape arising out of a nine-coordinate neodymium complex. The band shapes of the hypersensitive transition in any of the solvents used are distinctively different from typical band shape of eight- and ten-coordinate neodymium β-diketonate complexes [15–17, 19, 29, 39, 42–45]. The band shape is similar to nine-coordinate [Nd(hfaa)$_3$(tptz)] [18] and [Nd(tfaa)$_3$(tptz)] [46] in chloroform. It is strong evidence that this complex is nine-coordinate and retains its composition and structure in non-coordinating solvents. Since the tptz complex is more asymmetric, prominent Stark splitting appears in the band. The band shape of this transition in coordinating solvents is different from the band shape in non-coordinating solvents. Different band shapes demonstrate a change in the environment about Nd(III) which could be the result of complex–solvent interaction, leading to coordination of one solvent molecule. Coordination of donor solvents has been reported [39, 43, 46]. The band shape in coordinating solvents is

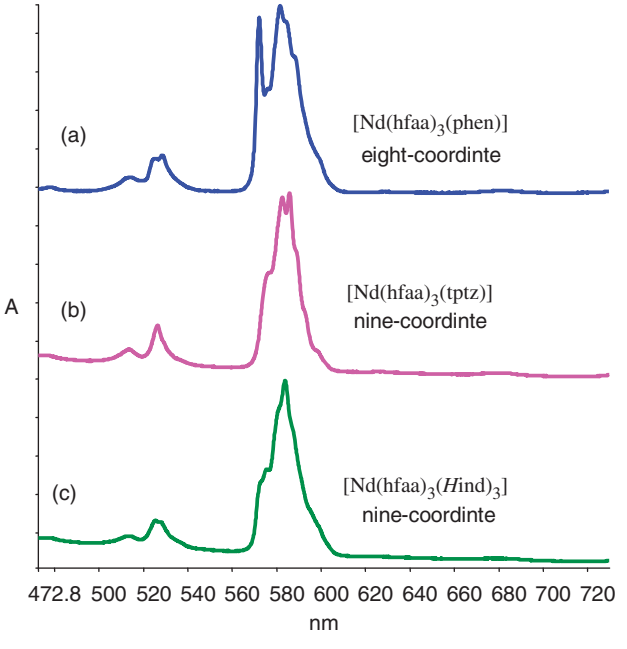

Figure 3. $^4G_{5/2}$, $^2G_{7/2} \leftarrow {}^4I_{9/2}$ hypersensitive transition of (a) eight-coordinate [Nd(hfaa)$_3$(phen)] (blue), (b) nine-coordinate [Nd(hfaa)$_3$(tptz)] (pink), and (c) nine-coordinate [Nd(hfaa)$_3$(*H*ind)$_3$] (green) in chloroform (concentration $= 5 \times 10^{-3}$ mol L^{-1}).

similar to the band shape of ten-coordinate $[Nd(hfaa)_3(phen)_2]$ [17] in chloroform and/or eight-coordinate β-diketonate complex in coordinating solvents (alcohols) [43, 46].

3.5.3. [Pr(hfaa)$_3$(Hind)$_3$]. Absorption spectra of the complex, in the visible region, display characteristic 4f–4f multiplet-to-multiplet transitions originating from the ground state $^3H_4$ of Pr(III). Only four transitions, $^1D_2$ (593 nm), $^3P_0$ (485 nm), $^3P_1 + {}^1I_6$ (472 nm), and $^3P_2$ (444 nm), are observed for the complex under study (figure S9 in the "Supplementary material" section). The oscillator strengths of the transitions of the complex in a series of non-aqueous solvents and hydrated $PrCl_3$ in water are given in table S1 in the "Supplementary material" section. The $^3F_2 \leftarrow {}^3H_4$ transition which appears in the near-infrared region, $\sim$5200 cm^{-1} (1923 nm), follows selection rules, $|\Delta J| \leq 2$, $|\Delta L| \leq 2$, and $\Delta S = 0$ for electric quadrupolar transitions, and is classified as being hypersensitive [38]. This transition could not be observed in this study due to inadequate range of the spectrophotometer. Of the four transitions, the $^3P_2$ is the most intense followed by $^3P_1$ while $^3P_0$ is the least intense. Only $^3P_2$ transition is sensitive to the change in solvent.

3.6. *Photoluminescence*

3.6.1. [Pr(hfaa)$_3$(*H*ind)$_3$]. Luminescence spectra of the praseodymium complex were recorded in a series of non-aqueous solvents: chloroform, benzene, acetonitrile, and pyridine (figure 4). Strong luminescence, upon excitation into the ligand absorption band, arises due to radiative f–f transitions originating from emitting levels of Pr(III) to their low lying states [47, 48]. The room temperature excitation spectrum of the

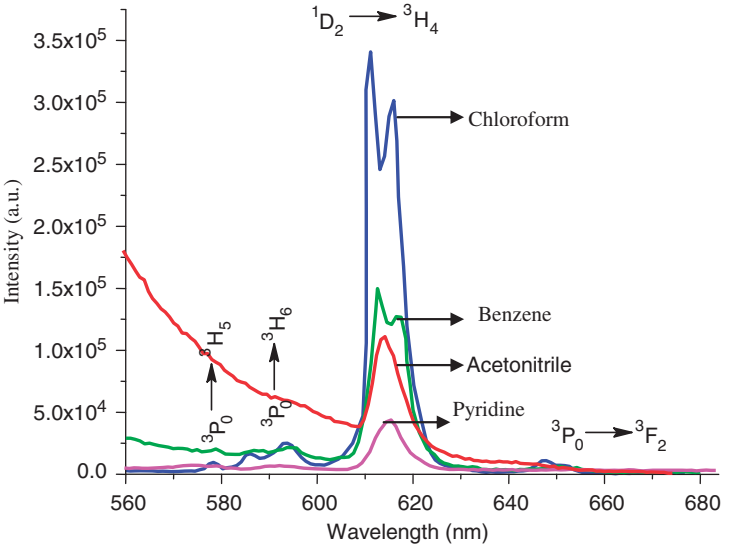

Figure 4. Emission spectra of $[Pr(hfaa)_3(Hind)_3]$ in different solvents (excitation = 360 nm; concentration = 5×10^{-2} mol L^{-1}) at room temperature.

praseodymium complex was obtained by monitoring the most intense emission observed in the visible region at 612 nm. The excitation spectrum consists of a broad band (200–400 nm) with maximum at 360 nm, which corresponds to excitation of the organic chromospheres (hfaa and *H*ind) and weak intraconfigurational f–f transitions from the $^3H_4$ ground state of Pr(III) (figure S10 in the "Supplementary material" section). Excitation spectra reveal that the energy transfer from the ligand to Pr(III) is efficient since S_0–S_1 excitation is dominant compared to weak f–f transitions.

Emission spectra of the complex in any of the solvents (figure 4) consists of four characteristic emission peaks of Pr(III) which are assigned to (a) $^3P_0 \rightarrow {}^3H_5$ (578 nm) (b) $^3P_0 \rightarrow {}^3H_6$ (593 nm) (c) $^1D_2 \rightarrow {}^3H_4$ (612 nm), and (d) $^3P_0 \rightarrow {}^3F_2$ (648 nm). The intense peak centered at 612 nm is mainly from $^1D_2 \rightarrow {}^3H_4$ transition, but is also believed to be overlapping with a weaker peak corresponding to the $^3P_0 \rightarrow {}^3H_6$ transition [49, 50]. The emission originates mainly from $^3P_0$ and $^1D_2$ levels *via* non-radiative relaxations from $^1I_6$ and $^3P_1$ states to these lower energy states. The strong luminescence observed for the complex reflects a good match between the ligand centered triplet and $^1D_2$ emissive state of Pr(III). There are four excited states that can efficiently receive energy from the triplet of hfaa ($E_T = 22{,}500\,cm^{-1}$) [51] and these are $^1I_6$ ($21{,}000\,cm^{-1}$), $^3P_1$ ($20{,}800\,cm^{-1}$), $^3P_0$ ($20{,}050\,cm^{-1}$), and $^1D_2$ ($16{,}500\,cm^{-1}$). The difference between the triplet state of hfaa and the emissive state ($^1D_2$) of Pr(III) is $\approx 6000\,cm^{-1}$, which is well suited for efficient energy transfer to Pr(III). The other three excited states ($^1I_6$, $^3P_1$, and $^3P_0$) are lower in energy than the triplet state of hfaa and may also receive energy from it, but intense emission is only observed from the $^1D_2$ level since the other excited state are too close in energy to the ligand centered triplet state. Thus, it can be postulated that non-radiative relaxation to $^1D_2$ from $^1I_6$, $^3P_1$, and $^3P_0$ prevails over back energy transfer to Pr(III) (figure 5).

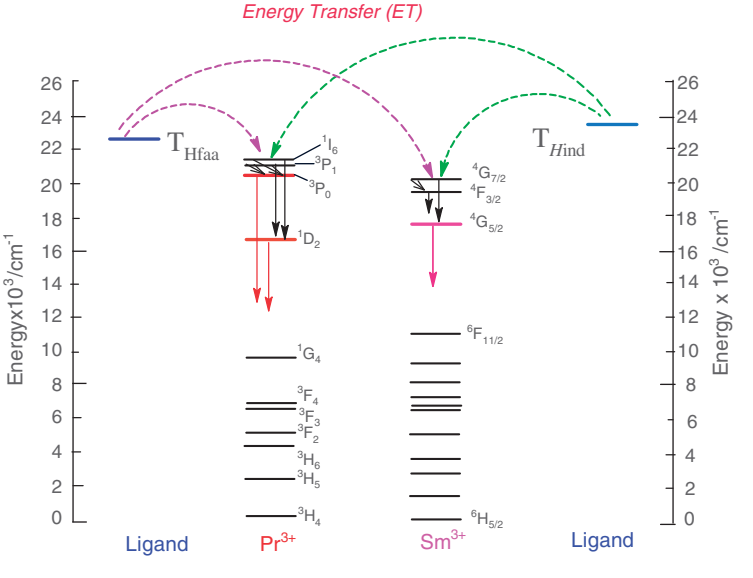

Figure 5. Energy level diagram of ligands and Ln(III) in [Ln(hfaa)$_3$(*H*ind)$_3$].

3.6.2. [Sm(hfaa)$_3$(*H*ind)$_3$]. The room temperature emission spectra of the samarium complex were recorded in different solvents (figure 6). The excitation spectrum (figure S11 in the "Supplementary material" section) of the Sm(III) complex (obtained by monitoring the most intense emission transition at 644 nm) contains a very intense broad band that corresponds to excitation of the organic chromophores ($S_0 \rightarrow S_1$) and several weak peaks that correspond to intraconfigurational 4f–4f transitions from the $^6H_{5/2}$ ground-state of Sm(III) to various excited states. Upon excitation of the ligand, intersystem crossing and energy transfer occur leading to Sm(III) luminescence. The strong ligand centered $S_0 \rightarrow S_1$ excitation band confirms that efficient energy transfer takes place from ligand to the emitting level of Sm(III). The emission spectrum displays three peaks, $^4G_{5/2} \rightarrow {}^6H_{5/2}$ (zero–zero band; 563 nm), $^4G_{5/2} \rightarrow {}^6H_{7/2}$ (magnetic dipole transition; 607 nm) and $^4G_{5/2} \rightarrow {}^6H_{9/2}$ (electric dipole transition; 644 nm), characteristic of Sm(III) in the region 520–680 nm. Of the three transitions, the electric dipole $^4G_{5/2} \rightarrow {}^6H_{9/2}$ hypersensitive transition is most intense, followed by $^4G_{5/2} \rightarrow {}^6H_{7/2}$ transition which shows Stark splitting at 597 and 619 nm. Furthermore, the bright-pink emission observed for the Sm(III) complex is reflective of a good match between the ligand-centered triplet states and the Sm(III) emissive states. The triplet energy state of hfaa lies near 22,500 cm^{-1}, well above the $^4G_{5/2}$ emitting state (17,900 cm^{-1}) of Sm(III). The energy gap between the two states ($\Delta E \sim 4600$ cm^{-1}) seems ideal for an efficient energy transfer to Sm(III). There are three Sm(III) excited states that can efficiently receive energy from the lowest triplet state of the ligands, and these are the $^4G_{7/2}$ ($\approx$20,050 cm^{-1}), $^4F_{3/2}$ ($\approx$8700 cm^{-1}), and $^4G_{5/2}$ ($\approx$7700 cm^{-1}) levels. Intense emission, however, is only observed from the $^4G_{5/2}$ level. The reason for this is the close proximity of these three excited states to each other, which causes electrons from the higher states to rapidly relax to the $^4G_{5/2}$ level from which radiative transitions occur [51].

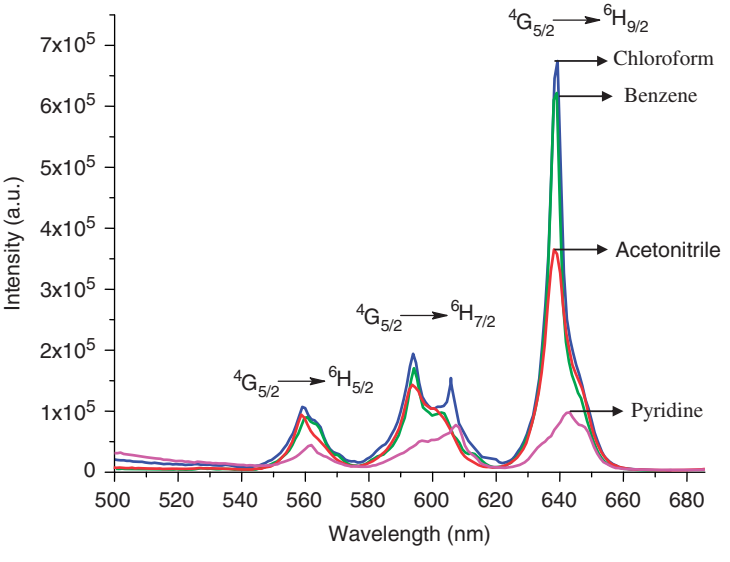

Figure 6. Emission spectra of [Sm(hfaa)$_3$(*H*ind)$_3$] in different solvents (excitation = 355 nm; concentration = 5×10^{-2} mol L^{-1}) at room temperature.

Table 4. Characteristics of the emission due to $^1D_2 \rightarrow {}^3H_4$ transition of $[Pr(hfaa)_3(Hind)_3]$ in various solvents.

Solvent	Peak wavelength (cm^{-1})	Fwhm[a] (nm)
Chloroform	16,340	9.24
Benzene	16,340	9.20
Acetonitrile	16,287	9.40
Pyridine	16,155	9.62

[a]Full-width at half-maximum of emission peak.

3.6.3. Solvent effect on luminescence properties. Luminescence intensity and band shape (figures 4 and 6) of the Pr and Sm complexes are sensitive to change in solvent. Emission spectra of Pr(III) and Sm(III) complexes are more spiked in chloroform and benzene (non-coordinating solvents) as compared to those in acetonitrile and pyridine, as indicated by the fwhm of the peaks. For instance, the fwhm of hypersensitive transition $^1D_2 \rightarrow {}^3H_4$ of Pr(III) complex follows the order: chloroform (9.24 nm) $\approx$ benzene (9.20 nm) $<$ acetonitrile (9.40 nm) $<$ pyridine (9.62 nm) (figure S12 in the "Supplementary material" section). Similarly, the fwhm of the hypersensitive transition $^4G_{5/2} \rightarrow {}^6H_{9/2}$ of Sm(III) complex in non-coordinating solvents are narrower (<5 nm) than those in coordinating ones (>5 nm) (figure S13 in the "Supplementary material" section), indicating monochromatic emission in non-coordinating solvents.

Magnetic dipole allowed transitions obey the selection rule, $\Delta J = 0 \pm 1$. Due to magnetic dipole character of the $^4G_{5/2} \rightarrow {}^6H_{5/2}$ transition ($\Delta J = 0$), the intensity is independent of the environment and can be used as a reference. The intensity parameter, η_{Sm}, which is the ratio between the area under the peaks of $^4G_{5/2} \rightarrow {}^6H_{9/2}$ and $^4G_{5/2} \rightarrow {}^6H_{5/2}$, is determined for this complex. The $^4G_{5/2} \rightarrow {}^6H_{9/2}$ is magnetic dipole forbidden and electric dipole allowed. Generally, the intensity ratio of electric dipole to magnetic dipole transitions has been used to measure the symmetry of the local environment around lanthanide. The higher intensity of an electric dipole transition indicates more asymmetry around the metal ion. The $^4G_{5/2} \rightarrow {}^6H_{7/2}$ transition is also magnetic dipole allowed but it is electric dipole dominated, therefore, its nature is partly a magnetic dipole and partly an electric dipole.

A comparison of experimental intensity parameter η_{Sm} for samarium complex in different solvents shows that luminescence intensity increases in the order pyridine $<$ acetonitrile $<$ benzene $<$ chloroform, illustrating the hypersensitive behavior of $^4G_{5/2} \rightarrow {}^6H_{9/2}$. This indicates that Sm(III) is in a highly polarizable environment. The η_{Sm} for Sm(III) complex in different solvents follows the order pyridine (2.61) $<$ acetonitrile (4.18) $<$ benzene (4.80) $<$ chloroform (5.21). The intensity of the transitions in non-coordinating solvents is higher than those in coordinating solvents (tables 4 and 5). Luminescence properties of lanthanide complexes are sensitive to variations in the symmetry of the coordination sphere around Ln(III). The higher luminescent intensity of the transitions of both the complexes and Stark splitting of the transitions ($^1D_2 \rightarrow {}^3H_4$ of Pr; $^4G_{5/2} \rightarrow {}^6H_{7/2}$ of Sm) is attributed to low molecular symmetry of these nine-coordinate complexes, as indicated by larger intensity parameter η_{Sm} in non-coordinating solvents. Furthermore, the magnitude of Stark splitting is larger in chloroform (C_{3V} symmetry) due to its low molecular symmetry than more symmetrical benzene (D_{6h}). Intensity of the transitions is lower and Stark splitting disappears in

Table 5. Characteristics of the emission transitions of [Sm(hfaa)$_3$(*H*ind)$_3$] in various solvents.

Solvent	Transitions $^4G_{5/2}\rightarrow$	Peak wavelength (cm^{-1})	Fwhm[a] (nm)	η_{Sm}[b]
Chloroform	$^6H_{9/2}$	15,528	4.96	5.21
	$^6H_{7/2}$	16,500	16.49	
	$^6H_{5/2}$	17,794	9.10	
Benzene	$^6H_{9/2}$	15,528	4.80	4.83
	$^6H_{7/2}$	16,750	16.12	
	$^6H_{5/2}$	17,794	9.09	
Acetonitrile	$^6H_{9/2}$	15,576	9.23	4.18
	$^6H_{7/2}$	16,778	18.06	
	$^6H_{5/2}$	17,857	9.11	
Pyridine	$^6H_{9/2}$	15,456	15.07	2.61
	$^6H_{7/2}$	16,529	21.28	
	$^6H_{5/2}$	17,762	9.13	

[a]Full-width at half-maximum of emission peak.
[b]Ratio of area under curves of the $^4G_{5/2}\rightarrow {}^6H_{9/2}$ (electric dipole transition) to the $^4G_{5/2}\rightarrow {}^6H_{5/2}$ (magnetic dipole transition) of Sm(III) complex.

coordinating solvents (acetonitrile and pyridine). The changes in luminescence intensity and band shape of the complexes can be attributed to the changes in the geometry of the complexes and symmetry of the field around Pr(III) and Sm(III). The 4f–4f transitions are forbidden for electric dipole radiations in a symmetric environment. Consequently, the lower intensity of the Pr(III) and Sm(III) complexes in a coordinating solvent could be related to a change in the structure in solution and could be explained by invoking coordination of one solvent molecule to Pr(III) and Sm(III) leading to more symmetric ten-coordinate geometry which leads to decrease in asymmetry of the ligand field around Ln(III). This decrease in asymmetry of the ligand field around Ln(III), due to coordination of solvent, decreases the radiative transition probability and as a result the emission intensity is lowered. These results are in agreement with observations noted on the oscillator strength of the hypersensitive transition in the 4f–4f absorption properties of the complex.

4. Conclusions

In an effort to synthesize seven-coordinate lanthanide complexes reaction of lanthanide chlorides, Hhfaa, and *H*ind in 1 : 3 : 1 or 1 : 3 : 3 molar ratio in ethanol yielded volatile and luminescent nine-coordinate complexes [Ln(hfaa)$_3$(*H*ind)$_3$]. The electronegative fluorines facilitate coordination of three *H*ind molecules. Opposite direction shifts of the methine and *H*ind protons indicate that the shifts are predominantly dipolar. The band shapes of the hypersensitive $^4G_{5/2}$, $^2G_{7/2}\leftarrow {}^4I_{9/2}$ transition in non-coordinating solvents are similar to the band shape of typical nine-coordinate β-diketone complexes. Coordinating solvents have pronounced impact on the band shape and oscillator strength of the transitions; the band shape of the hypersensitive transition in the coordinating solvents resembles the band shape of ten-coordinate complexes. Luminescence intensities are higher and the bands show Stark splitting in non-coordinating solvents, while in coordinating solvent decrease in luminescence intensity and disappearance of Stark splitting are observed. The higher values of experimental

intensity parameter (η_{Sm}) for samarium complex in non-coordinating solvents indicate increased asymmetry around Sm(III). The low melting point and volatility of the complexes are advantageous for their use as precursors for high-performance lanthanide-based materials through chemical vapor deposition. Thin films can also be generated from these luminescent complexes and used in fabricating light-emitting devices operated at lower temperatures.

Acknowledgements

This research was supported in part by the UGC Special Assistance Programme of the Department of Chemistry (No. F.540/17/DRS/2007/SAP-1). We thank Prof. Bachcha Singh, Head, Department of Chemistry, Banaras Hindu University, Varanasi, for his help in getting the microanalysis and Mr Avatar Singh, SAIF, Panjab University, Chandigarh, for recording NMR spectra of the complexes.

References

[1] J.M. Lehn. *Angew. Chem., Int. Ed. Engl.*, **29**, 1304 (1990) and references therein.
[2] J.C.G. Bunzli. In *Lanthanide Probes in Life, Chemical and Earth Sciences, Theory and Practice*, J.C.G. Bunzli, G.R. Choppin (Eds), Amsterdam, Elsevier (1989).
[3] E.G. Moore, A.P.S. Samuel, K.N. Raymond. *Acc. Chem. Res.*, **42**, 542 (2009).
[4] M.J. Weber. In *Handbook on the Physics and Chemistry of Rare Earths*, K.A. Gschneidner Jr, L.R. Eyring (Eds), Vol. 4, p. 275, North-Holland, Amsterdam (1979).
[5] D. Parker. *Coord. Chem. Rev.*, **205**, 109 (2002).
[6] V.W.W. Yam, K.K.W. Lo. *Coord. Chem. Rev.*, **184**, 157 (1999).
[7] J. Kido, Y. Okamoto. *Chem. Rev.*, **102**, 2357 (2002).
[8] G. Zucchi, T. Jeon, D. Tondelier, D. Aldakov, P. Thuéry, M. Ephritikhine, B. Geffroy. *J. Mater. Chem.*, **20**, 2114 (2010).
[9] J.-C. Bunzli, C. Piguet. *Chem. Soc. Rev.*, **34**, 1048 (2005).
[10] K. Binnemans. *Chem. Rev.*, **109**, 4283 (2009).
[11] G.F. de Sa, O.L. Malta, C. de Mello Donega, A.M. Simas, R.L. Longo, P.A. Santa-Cruz, E.F. da Silva. *Coord. Chem. Rev.*, **196**, 165 (2000) and references therein.
[12] L.R. Melby, N.J. Rose, E. Abramson, J.C. Caris. *J. Am. Chem. Soc.*, **86**, 5117 (1964).
[13] K. Iftikhar, M. Sayeed, N. Ahmad. *Inorg. Chem.*, **21**, 80 (1982).
[14] D.R. van Staveren, G.A. van Albada, J.G. Haasnoot, H. Kooijman, A.M.M. Lanfredi, P.J. Nieuwenhuizen, A.L. Spek, F. Ugozzoli, T. Weyhermüller, J. Reedijk. *Inorg. Chim. Acta*, **315**, 163 (2001).
[15] M. Irfanullah, K. Iftikhar. *Inorg. Chem. Commun.*, **12**, 296 (2009).
[16] M. Irfanullah, K. Iftikhar. *Inorg. Chem. Commun.*, **13**, 694 (2010).
[17] Z. Ahmed, K. Iftikhar. *Inorg. Chim. Acta*, **393**, 2609 (2010).
[18] Z. Ahmed, K. Iftikhar. *Inorg. Chem. Commun.*, **13**, 1253 (2010).
[19] R. Ilmi, K. Iftikhar. *Inorg. Chem. Commun.*, **13**, 1552 (2010).
[20] A. Bellusci, G. Barberio, A.G. Crispini, M. Ghedini, M. La Deda, D. Pucci. *Inorg. Chem.*, **44**, 1818 (2005).
[21] O.L. Malta, H.F. Brito, J.F.S. Menezes, F.R. Goncalves e Silva, C. de Mello Donega, S. Alves Jr. *Chem. Phys. Lett.*, **282**, 233 (1998).
[22] S.V. Eliseeva, J.-C.G. Bunzli. *Chem. Soc. Rev.*, **39**, 189 (2010).
[23] J.-C.G. Bunzli. *Chem. Rev.*, **110**, 2729 (2010).
[24] R. Liu, L. Li, X. Wang, P. Yang, C. Wang, D. Liao, J.-P. Sutter. *Chem. Commun.*, **46**, 2566 (2010).
[25] M.D. Allendorf, C.A. Bauer, R.K. Bhakta, R.J.K. Houk. *Chem. Soc. Rev.*, **38**, 1330 (2009).
[26] J. Catalan, J.C. del Valle, R.M. Claramunt, G. Boyer, J. Laynez, J. Gomez, P. Jimenez, F. Tomas, J. Elguero. *J. Phys Chem.*, **98**, 10 606 (1994).

[27] I.N. Stepanenko, A.A. Krokhin, R.O. John, A. Roller, V.B. Arion, M.A. Jakupec, B.K. Keppler. *Inorg. Chem.*, **47**, 7338 (2008).
[28] K. Iftikhar, M. Sayeed, N. Ahmed. *Bull. Chem. Soc. Japan*, **55**, 2258 (1982).
[29] K. Iftikhar, N. Ahmad. *Polyhedron*, **4**, 333 (1985).
[30] M.F. Richardson, R.E. Sievers. *Inorg. Chem.*, **10**, 498 (1971).
[31] P. Thakur, V. Chakravortty, K.C. Dash. *Polyhedron*, **16**, 1417 (1997).
[32] A.P. Hunter, A.M.J. Lees, A.W.G. Platt. *Polyhedron*, **26**, 4865 (2007).
[33] J. Zhang, P.D. Badger, S.J. Geib, S. Petoud. *Inorg. Chem.*, **46**, 6473 (2007).
[34] K. Iftikhar. *Polyhedron*, **15**, 1113 (1996).
[35] W.T. Carnell, P.R. Feilds, K. Rajnak. *J. Chem. Phys.*, **49**, 4424 (1968).
[36] A.A. Khan, H.A. Hussain, K. Iftikhar. *Spectrochim. Acta, Part A*, **59**, 1051 (2003).
[37] R.D. Peacock. *Struct. Bond.*, **22**, 83 (1975).
[38] D.E. Henrie, R.L. Fellows, G.R. Choppin. *Coord. Chem. Rev.*, **18**, 199 (1976).
[39] A.A. Ansari, M. Irfanullah, K. Iftikhar. *Spectrochim. Acta, Part A*, **67**, 1178 (2007).
[40] A.A. Khan, K. Iftikhar. *Polyhedron*, **16**, 4153 (1997).
[41] D.G. Karrakar. *Inorg. Chem.*, **6**, 1863 (1967).
[42] A.A. Ansari, H.A. Hussain, K. Iftikhar. *Spectrochim. Acta, Part A*, **68**, 1305 (2007).
[43] A.A. Ansari, R. Ilmi, K. Iftikhar. *J. Lumin.*, **132**, 51 (2012).
[44] D.E. Henrie, G.R. Choppin. *J. Chem. Phys.*, **49**, 477 (1968).
[45] M. Irfanullah, K. Iftikhar. *Inorg. Chem. Commun.*, **13**, 1234 (2010).
[46] R. Ilmi, K. Iftikhar. *J. Coord. Chem.*, **65**, 403 (2012).
[47] K. Binnemans, C. Görller-Walrand. *Chem. Rev.*, **102**, 2303 (2002).
[48] K. Binnemans. In *Handbook on the Physics and Chemistry of Rare Earths*, K.A. Gschneidner Jr, J.-C.G. Bünzli, V.K. Pecharsky (Eds), Vol. 35, Chap. 225, p. 107, Elsevier, Amsterdam (2005).
[49] M.D. Regulacio, M.H. Pablico, J.A. Vasquez, P.N. Myers, S. Gentry, M. Prushan, S.-W. Tam-Chang, S.L. Stoll. *Inorg. Chem.*, **47**, 1512 (2008).
[50] Y.-L. Huang, M.-Y. Huang, T.-H. Chan, B.-C. Chang, K.-H. Lii. *Chem. Mater.*, **19**, 3232 (2007).
[51] S.B. Meshkova, A.V. Kiriak, Z.M. Topilova, A.M. Andrianov. *Russ. J. Inorg. Chem.*, **52**, 556 (2007).